Wave- and Wind-Driven Flow in Water of Finite Depth

ZHIGANG XU AND A. J. BOWEN

Department of Oceanography, Dalhousie University, Halifax, Nova Scotia, Canada

(Manuscript received 16 December 1992, in final form 24 August 1993)

ABSTRACT

The authors first derive both Coriolis-induced and viscosity-induced stresses for arbitrary water depth and arbitrary wave direction. Opportunity is taken here to succinctly and rigorously derive the Longuet-Higgins virtual tangential stress due to wave motion. It is shown that the virtual stress is a projection on the surface slope of two viscous normal stresses acting on the vertical and horizontal planes. Then a simple Eulerian model is presented for the steady flow driven by waves and by waves and winds. This simple Eulerian model demonstrates that the wave forcing can be easily incorporated with other conventional forcing, rather than resorting to a complicated and lengthy perturbation analysis of the Lagrangian equations of motion. A further focus is given to the wave-driven flow when the various limits of the wave-driven steady flow are discussed. The wave-driven steady flow given by the model yields a unified formula between Ursell and Hasselmann's inviscid but rotational theory and the Longuet-Higgins viscid but nonrotational theory, and it becomes an Eulerian counterpart of Madsen's deep-water solution when the deep-water limit is taken. The model is further expanded for the case of unsteady wave forcing, yielding a general formula for any type of time variation in the wave field. Two examples are considered: a suddenly imposed wave field that is then maintained steady and a suddenly imposed wave field that is then subject to internal and bottom frictional decay. The extension of these results to the case of random waves is briefly discussed. Finally, an example is presented that suggests the need to add surface wave forcing in classical shelf dynamics.

1. Introduction

Stokes (1847) established a theory for wave-induced mean flow, which predicts that for a periodic surface wave field there is an associated mean flow in the direction of wave propagation. Since this mean flow can be responsible for a net material transport of sediments, oil slicks, etc., the concept, which came to be known as Stokes drift, has been widely applied in the real ocean. Not until 1950 did Ursell question the application of Stokes' theory, which was originally derived from a nonrotation frame, to the rotating ocean. He argued, from the point of view of absolute circulation conservation, that it is impossible for a steady wave field to produce a steady Lagrangian mean (Fig. 1). Pollard (1970) then examined the wave problem in rotational Lagrangian coordinates showing that each water particle in wave motion experiences an exactly circular orbit so that there is no net material transport, confirming Ursell's theory.

Hasselmann (1970) retained the Coriolis force in calculating the wave-induced Reynolds stress tensor and found that, when the earth's rotation is taken into account, the horizontal wave orbital velocity component is no longer in quadrature with its vertical counterpart; therefore a mean shear component of the Reynolds stress tensor arises. The associated body force exerted by the waves is $-\mathbf{f} \times \mathbf{u}_{st}$, where $\mathbf{f}$ is the Coriolis vector and $\mathbf{u}_{st}$ is the Stokes drift velocity. A steady response of a laterally homogeneous ocean to this body force is an Eulerian current $\mathbf{u}_e$ equal and opposite to the Stokes drift, resulting in the zero Lagrangian mean required by Ursell's theory. The surprising result is that a high-frequency surface gravity wave field produces shear stresses in the water column due to the earth's rotation. As will be shown later, for a simple wave train, the Coriolis-induced wave stress at the surface can be expressed as $\rho a^2 \sigma f/2$ in deep water where ρ is the density of seawater, a is the wave amplitude, σ is the wave frequency, and f is the Coriolis parameter; so if $a = \sqrt{2}m$, $\sigma = 1\ \mathrm{s}^{-1}$, $f = 10^{-4}\ \mathrm{s}^{-1}$, and $\rho = 10^3\ \mathrm{kg\ m}^{-3}$, then the stress is 0.1 Pa, which is of the order of a typical wind stress. For a rough sea, the shear stress can be much larger.

In a nonrotating frame, Longuet-Higgins (1953, 1960) showed that two thin viscous wave boundary layers, at the surface and at the bottom, can strongly influence the mass transport in the interior region, no matter how small the viscosity. This influence can be expressed in terms of two boundary conditions: a steady bottom streaming and a surface virtual tangential stress. Predictions using the formula for viscous wave mass transport obtained by Longuet-Higgins yields good

Corresponding author address: Dr. Zhigang Xu, Department of Oceanography, Dalhousie University, Halifax, Nova Scotia B3H 4J1, Canada.

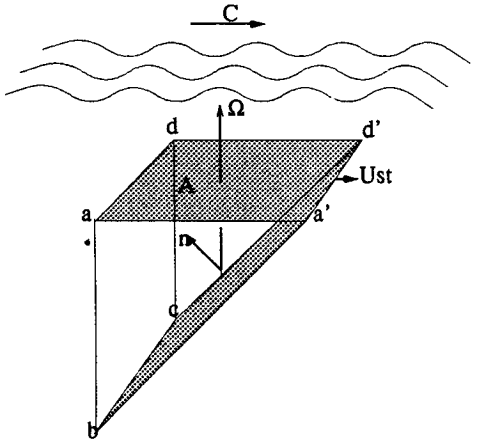

FIG. 1. Diagram of Ursell's argument: If there was a steady Lagrangian mean, denoted by U_{st}, then the area projection, **A**, of a circuit would increase unboundedly and so would the number of the captured planetary vorticity filaments, denoted by Ω, which would lead an infinitely large relative circulation around the circuit **ba'd'cb**, which initially coincided with **badc**, and would result in an infinitely large velocity along the side **d'a'** with finite length.

agreement with wave tank data, while Stokes drift theory does not.

Thus Stokes drift theory is markedly modified by two different approaches: Ursell's and Hasselmann's inviscid but rotational approach and the Longuet-Higgins viscid but nonrotational approach. In a realistic ocean, one should therefore consider both rotation and fluid viscosity in addressing the wave-induced flow problem. Madsen (1978), followed by Weber (1983a,b) and Jenkins (1986, 1987a,b), combined the Coriolis effect and fluid viscosity in wave mass transport in deep water, and successfully removed the so-called Longuet-Higgins paradox in deep water. The paradox, which was raised first by Huang (1970), arises simply because the virtual tangential stress remains unbalanced in a nonrotational deep water for steady flow. In the models of Madsen (1978) and Weber (1983a,b), the eddy viscosity was treated to be constant and waves to be monochromatic. Jenkins (1987a,b; 1989) developed models for vertical varying eddy viscosity and for the random wave case. Recently, Weber and Melson (1993a,b) considered the effects of growing/breaking waves on the mass transport.

However, no one seems to have extended the work of Madsen, Weber, and Jenkins to shallow water where the surface waves may influence the whole water column. For example, swell of about 20 sec period can influence the whole water depth of about 200 m (Grant et al. 1984). During periods of large swell, it seems unlikely that any dynamic model whose aim is to forecast or hindcast the real flow can neglect the wave stress. The purpose of this paper, therefore, is to present a simple Eulerian model to yield the wind- and wave-driven flow in water of finite depth. Such a model should be of value in interpreting the observed flow on the shelf.

In the wave mass transport problem, the Lagrangian description is often favored (Ünlüata and Mei 1970; Madsen 1978; Weber 1983a,b; Jenkins 1986, 1987a,b). The choice of the Lagrangian description brings in an evident convenience, that is, to turn the fluctuating free surface into a fixed plane, which is desirable for those models designed to yield the detailed structure of the surface boundary layer. However, the choice makes the equations of motion and the algebra lengthy and complicated. Given that it is desirable to make a comparison between the results of a model including wave forcing and that with only the conventional wind forcing where Eulerian description is overwhelmingly used, we have chosen the Eulerian description for our model. After we get the result from the Eulerian model, for the purpose of comparison with the previous results in the Lagrangian description, we can employ a simple relationship of $\langle u_l \rangle = \langle u_e \rangle + u_{st}$, where $\langle u_l \rangle$ is the Lagrangian mean and $\langle u_e \rangle$ the Eulerian mean and u_{st} the Stokes drift (e.g., Longuet-Higgins 1969a). For a general dynamic link between the two descriptions, reference is made to Andrews and McIntyre (1978). Weber (1990) also gave a comparison of the two approaches for the wave mass transport problem in deep rotating water.

2. Primary wave motion and secondary wave stress

a. Inviscid primary wave motion in the interior region and the Coriolis-induced wave stress

Hasselmann (1970) derived the Coriolis-induced wave stress without resorting to any specific wave solution. His derivation is general, but also makes the generating mechanism of the stress less evident. In the following, we provide a finite water wave solution in a rotating system from which one can see the generating mechanism of the stress more clearly and can immediately work out the stress formula in terms of the wave parameters.

For the first-order wave motion, a frictionless model is a reasonable approximation for the interior region in a rotating Cartesian frame with angular frequency of $f/2$,

$$\frac{\partial \tilde{u}}{\partial t} - f\tilde{v} = -\frac{1}{\rho}\frac{\partial \tilde{p}}{\partial x} \tag{1}$$

$$\frac{\partial \tilde{v}}{\partial t} + f\tilde{u} = 0 \tag{2}$$

$$\frac{\partial \tilde{w}}{\partial t} + g = -\frac{1}{\rho}\frac{\partial \tilde{p}}{\partial z} \tag{3}$$

$$\frac{\partial \tilde{u}}{\partial x} + \frac{\partial \tilde{w}}{\partial z} = 0, \tag{4}$$

subject to

$$\tilde{w} = 0 \quad \text{at} \quad z = -h \tag{5}$$

$$\tilde{p} = 0 \quad \text{at} \quad z = \tilde{\eta}, \tag{6}$$

where the x axis is taken to be the direction of wave propagation, the y axis is parallel with wave crests, and z is taken to be vertically upward measured from the mean sea surface (Fig. 2).

Seeking a plane wave solution to the above model, one finds that

$$\tilde{u} = \frac{\lambda a\sigma}{k} \frac{\cosh(\lambda h + \lambda z)}{\sinh\lambda h} \cos(kx - \sigma t) \tag{7}$$

$$\tilde{v} = \left(\frac{f}{\sigma}\right) \frac{\lambda a\sigma}{k} \frac{\cosh(\lambda h + \lambda z)}{\sinh\lambda h} \sin(kx - \sigma t) \tag{8}$$

$$\tilde{w} = a\sigma \frac{\sinh(\lambda h + \lambda z)}{\sinh\lambda h} \sin(kx - \sigma t) \tag{9}$$

$$\tilde{p} = \rho g a \frac{\cosh(\lambda h + \lambda z)}{\cosh\lambda h} \cos(kx - \sigma t) - \rho g z \tag{10}$$

$$\tilde{\eta} = a \cos(kx - \sigma t), \tag{11}$$

in which k is the wavenumber, $\lambda = k/\sqrt{1 - (f/\sigma)^2}$, and $\sigma^2 = g\lambda \tanh\lambda h$. In Weber's (1990) paper, which gives a comparison of the Eulerian and the Lagrangian approaches for the wave drift problem in a rotating ocean, an Eulerian deep-water wave solution is presented. The solution shown above is more general, in which the deep-water solution is included as its limit when $h \to \infty$. Also, the solution here so far is exact. No demand has been put on the ratio of σ/f. Of course, substitution of the practical numbers of σ and f will make the σ^2/f^2, which appears in the expression of λ, to be of order of $O(10^{-8})$, which is insignificant in our problem. Therefore, in the following discussion we will approximate λ with k.

The significance of the rotating frame to the wave solution is that it introduces a crest parallel wave orbital velocity component, $\tilde{v}$. This component is in phase with its vertical counterpart, $\tilde{w}$. A net wave-induced Reynolds stress then arises from averaging over a wave cycle,

$$-\rho\langle\tilde{v}\tilde{w}\rangle = -\rho a^2 f\sigma \frac{\sinh 2k(h + z)}{4\sinh^2(kh)}, \tag{12}$$

where the angle bracket means time average over a wave period. For those hyperbolic functions in (7) $\sim$ (10), z is defined from $z = 0$ to $z = -h$ instead of from $z = \tilde{\eta}$ to $z = -h$. This involves an assumption that the wave solutions can be analytically extended to the mean sea surface when $\tilde{\eta} < 0$, which is a usual assumption in linear wave theory [e.g., Phillips 1977, Eqs. (3.1.10 $\sim$ 11); Hasselmann 1970, p. 192; Weber and Melson 1993a, Eq. (20)]. Consequently, the derived stress of (12) is also defined from the mean sea level $z = 0$ to the sea bed $z = -h$.

To estimate the size of this stress, we consider the deep-water case. In deep water, the above stress becomes

$$\rho\langle\tilde{v}\tilde{w}\rangle = \rho \frac{a^2 f\sigma}{2} e^{2kz}. \tag{13}$$

If we put $f = 10^{-4}\ \text{s}^{-1}$, $\rho = 10^3\ \text{kg m}^{-3}$, $\sigma = 1\ \text{s}^{-1}$, and $a = \sqrt{2}$ m, which correspond only to moderate waves, then the above stress yields a value of 0.1 Pa at the surface, which is the size of a typical wind stress.

Since a surface wave decays vertically, as its name suggests, one can calculate an associated body force by taking a derivative of (12) with respect to the vertical coordinate z. The body force is then

$$-\rho \frac{\partial\langle\tilde{v}\tilde{w}\rangle}{\partial z} = -\rho \frac{a^2 f\sigma}{\delta_{st}} \frac{\cosh 2k(h + z)}{4\sinh^2(kh)}$$

$$= -f\rho u_{st}, \tag{14}$$

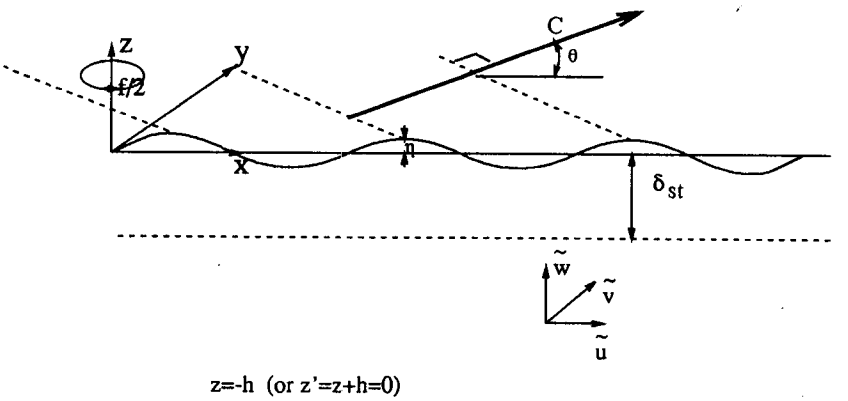

FIG. 2. Eulerian coordinates for the wave problem in a rotating water with an arbitrary depth. In getting the solution for $\tilde{u}$, $\tilde{v}$, $\tilde{w}$, $\tilde{p}$, and $\tilde{\eta}$, we assume $\theta = 0$ for simplicity, and afterward we relax this assumption.

where $\delta_{st} = 1/(2k)$ and is known as the Stokes depth (Fig. 2), and u_{st} denotes the Stokes velocity

$$u_{st} = \sigma a^2 k \frac{\cosh 2k(h+z)}{2\sinh^2(kh)}. \quad (15)$$

In the above we have assumed for simplicity that the wave propagation direction coincides with positive x direction. If the wave direction is at an arbitrary angle θ with respect to the x axis (Fig. 2), it is not difficult to work out the body force as

$$-\rho \mathbf{f} \times \mathbf{u}_{st}, \quad (16)$$

or, written in a complex plane,

$$\rho \frac{a^2 f\sigma}{\delta_{st}} \frac{\cosh 2(kh+kz)}{4\sinh^2(kh)} e^{i(\theta-\pi/2)}, \quad (17)$$

where k is now the wavenumber in the direction of θ. Note that a train of shoreward waves produces an alongshore force.

b. *Wave-induced virtual tangential stress on the free surface*

In a nonrotating frame, Longuet-Higgins (1953) Longuet-Higgins and Stewart (1960) showed that the two thin wave boundary layers have fundamental effects on the wave mass transport in the interior region no matter how small the viscosity. The effects can be expressed as two boundary conditions just beneath a thin free surface boundary layer and just above a thin bottom boundary layer, respectively. [The wave boundary layers are practically millimeter order thick, e.g., Russell and Osorio (1958).] Written in an Eulerian sense, they are

$$\mu \frac{\partial \langle u \rangle}{\partial z} = 2\mu\sigma a^2 k^2 \coth kh \quad \text{at} \quad z = 0 - \beta^{-1} \approx 0 \quad (18)$$

$$\langle u \rangle = \frac{3\sigma a^2 k}{4\sinh^2 kh} \overset{or}{=} \frac{3}{2} u_{st}(-h) \quad \text{at}$$

$$z = -h + \beta^{-1} \approx -h, \quad (19)$$

where the wave propagation is again in the x direction. Equation (18) has been termed as wave-induced virtual tangential stress and (19) bottom streaming ($\beta = \sqrt{\sigma/2\nu}$, ν is kinematic viscosity and σ wave frequency).

Of the two boundary conditions, the one near the free surface has drawn considerable discussions (e.g., Phillips 1977; Longuet-Higgins 1969b; Huang 1970; Ünlüata and Mei 1970; and Weber 1983a) because of its important role in the transfer of wave energy into mean flow and yet, while it seems sensible there should be a stress, the details of the mechanism are far from obvious. The complexity in the mathematical derivation given by Longuet-Higgins masks the generating mechanism. Phillips (1977) offered an explanation from the point of view of wave energy dissipation into the surrounding water. The extension of this energy approach to the rotating system is presented in the appendix to this paper. However, using energy to account for a stress is not really adequate, simply because an energy is scalar and a stress is a vector. Here, we take this opportunity to present a succinct and rigorous way to derive the Longuet-Higgins wave-induced virtual tangential stress. As is shown below, our derivation reveals that the virtual stress can be derived by considering projections on the surface slope of two viscous normal stress acting on the two axis planes, respectively.

Let

$$F = z - a\cos(kx - \sigma t); \quad (20)$$

then the free surface is described by

$$F \equiv 0 \quad (21)$$

and the outward normal direction at a point O on the free surface (Fig. 3) is

$$\mathbf{n} = [n_x, n_z] = \frac{\nabla F}{|\nabla F|} \approx \left[ka\sin\phi,\ 1 - \frac{1}{2}(ka)^2\sin^2\phi\right], \quad \text{omit } O[(ka)^3], \quad (22)$$

where we have used ϕ to denote $kx - \sigma t$. The tangential direction $\mathbf{s}$ at the point O is

$$\mathbf{s} = [n_z, -n_x] = \left[1 - \frac{1}{2}(ka)^2\sin^2\phi,\ -ka\sin\phi\right]. \quad (23)$$

Calculate tangential stress, P_{ns}, at the point O on the free surface as follows:

$$P_{ns} = n_i P_{ij} s_j \quad (i = x, z \quad j = x, z)$$
$$\approx P_{zx} + ka\sin\phi[P_{xx} - P_{zz}] - 2(ka)^2\sin^2\phi P_{xz}, \quad \text{omit } O[(ka)^3]. \quad (24)$$

On the free surface P_{ns} vanishes, thus from (24)

$$P_{zx} + ka\sin\phi[P_{xx} - P_{zz}] - 2(ka)^2\sin^2\phi P_{xz} = 0. \quad (25)$$

The relationship between stress tensor and strain of motion is

$$P_{xx} = -p + 2\mu\frac{\partial u}{\partial x} \quad (26)$$

$$P_{zx} = \mu\left(\frac{\partial u}{\partial z} + \frac{\partial w}{\partial x}\right) \quad (27)$$

$$P_{zz} = -p + 2\mu\frac{\partial w}{\partial z}. \quad (28)$$

Assume that

$$u = \epsilon u_1 + \epsilon^2 u_2 + \cdots \tag{29}$$

$$w = \epsilon w_1 + \epsilon^2 w_2 + \cdots \tag{30}$$

in which ϵ is a small parameter, and the first-order u_1, w_1 are high-frequency periodic surface wave motion and the second and higher orders are much lower-frequency motion. In the problem of wave-driven flow, it is proper to take

$$\epsilon = ka. \tag{31}$$

Accordingly,

$$P_{xx} = -p + (ka)2\mu \frac{\partial u_1}{\partial x} + (ka)^2 2\mu \frac{\partial u_2}{\partial x} + \cdots \tag{32}$$

$$P_{zx} = (ka)\mu\left(\frac{\partial u_1}{\partial z} + \frac{\partial w_1}{\partial x}\right) + (ka)^2\mu \frac{\partial u_2}{\partial z} + \cdots \tag{33}$$

$$P_{zz} = -p + (ka)2\mu \frac{\partial w_1}{\partial z} + (ka)^2\mu \frac{\partial w_2}{\partial z} + \cdots, \tag{34}$$

where we have dropped off $\partial w_2/\partial x$ from P_{zx} because of the horizontal scale in which second-order motion varies is much larger than the water depth in the ocean, as is commonly assumed. Substitution of (32), (33), and (34) into (25) yields

$$(ka)\mu\left(\frac{\partial u_1}{\partial z} + \frac{\partial w_1}{\partial x}\right) + (ka)^2\left[2\mu \sin\phi\left(\frac{\partial u_1}{\partial x} - \frac{\partial w_1}{\partial z}\right) + \mu \frac{\partial u_2}{\partial z}\right] + \cdots = 0. \tag{35}$$

For the above equation to hold, the coefficients of each power of (ka) must equal zero; that is,

$$\mu\left(\frac{\partial u_1}{\partial z} + \frac{\partial w_1}{\partial x}\right) = 0 \tag{36}$$

$$\left[2\mu \sin\phi\left(\frac{\partial u_1}{\partial x} - \frac{\partial w_1}{\partial z}\right) + \mu \frac{\partial u_2}{\partial z}\right] = 0 \tag{37}$$

$$\cdots \tag{38}$$

Averaging (37) yields

$$\mu\left\langle \frac{\partial u_2}{\partial z} \right\rangle = -2\mu\left\langle \sin\phi\left(\frac{\partial u_1}{\partial x} - \frac{\partial w_1}{\partial z}\right)\right\rangle, \tag{39}$$

while averaging (29) yields

$$\langle u \rangle = (ka)^2 \langle u_2 \rangle + \mathrm{O}[(ka)^3]. \tag{40}$$

The combination of (39) and (40) then results in

$$\mu \frac{\partial \langle u \rangle}{\partial z} = -(ka)^2\left\langle 2\mu \sin\phi\left(\frac{\partial u_1}{\partial x} - \frac{\partial w_1}{\partial z}\right)\right\rangle, \tag{41}$$

where terms of $\mathrm{O}[(ka)^3]$ have been dropped. This equation reveals the essence of the virtual tangential stress: It is the projection on the surface slope of two viscous normal stresses acting on the two axis planes, respectively (Fig. 3).

The next question is how to calculate the virtual tangential stress if we are provided only with the inviscid wave solution. This can be done as follows. First we notice that

$$\frac{\partial u_1}{\partial x} - \frac{\partial w_1}{\partial z} = 2\frac{\partial u_1}{\partial x} \tag{42}$$

because of incompressibility of the fluid. Second, we define two components in u_1 near the free surface, one is inviscid solution, say $u_{1\mathrm{invis}}$, and one is viscid solution, say $u_{1\mathrm{vis}}$. Although we do not know the details about $u_{1\mathrm{vis}}$, one thing about it is certain: $u_{1\mathrm{vis}} = \mathrm{O}(k/\beta)u_{1\mathrm{invis}}$ ($\beta^{-1} = \sqrt{2\nu/\sigma}$ is the thickness of the surface viscous boundary layer) for on the free surface the shear stress due to the inviscid motion must be balanced by that due to the viscid motion. Because of the high-frequency of the first-order motion, the thickness of the viscous boundary layer is much smaller than the wave length; that is,

$$\frac{k}{\beta} \ll 1. \tag{43}$$

Thus, one can calculate the virtual stress by using only inviscid solution:

$$\frac{\partial u_1}{\partial x} - \frac{\partial w_1}{\partial z} = 2\frac{\partial u_1}{\partial x} = 2\frac{\partial u_{1\mathrm{invis}}}{\partial x}\left[1 + \mathrm{O}\left(\frac{k}{\beta}\right)\right]; \tag{44}$$

substitution of (44) into (41) yields

$$\mu \frac{\partial \langle u \rangle}{\partial z} = -4\mu(ka)^2\left\langle \sin\phi \frac{\partial u_{1\mathrm{invis}}}{\partial x}\right\rangle, \quad \text{omit } \mathrm{O}\left[(ka)^2 \frac{k}{\beta}\right]. \tag{45}$$

The inviscid solution to the surface gravity wave motion in a nonrotating shallow water is

$$u_{\mathrm{invis}} = (ka)\frac{g}{\sigma}\frac{\cosh(kh + kz)}{\cosh kh}\cos\phi = (ka)u_{1\mathrm{invis}} \tag{46}$$

(e.g., Phillips 1977). Thus, substituting

$$u_{1\mathrm{invis}} = \frac{g}{\sigma}\frac{\cosh(kh + kz)}{\cosh kh}\cos\phi \tag{47}$$

into (45), we obtain the virtual stress

$$\mu \frac{\partial \langle u \rangle}{\partial z} = 2\mu(ka)^2\sigma \coth kh, \tag{48}$$

where the dispersion relationship $\sigma^2 = gk \tanh(kh)$ has been used.

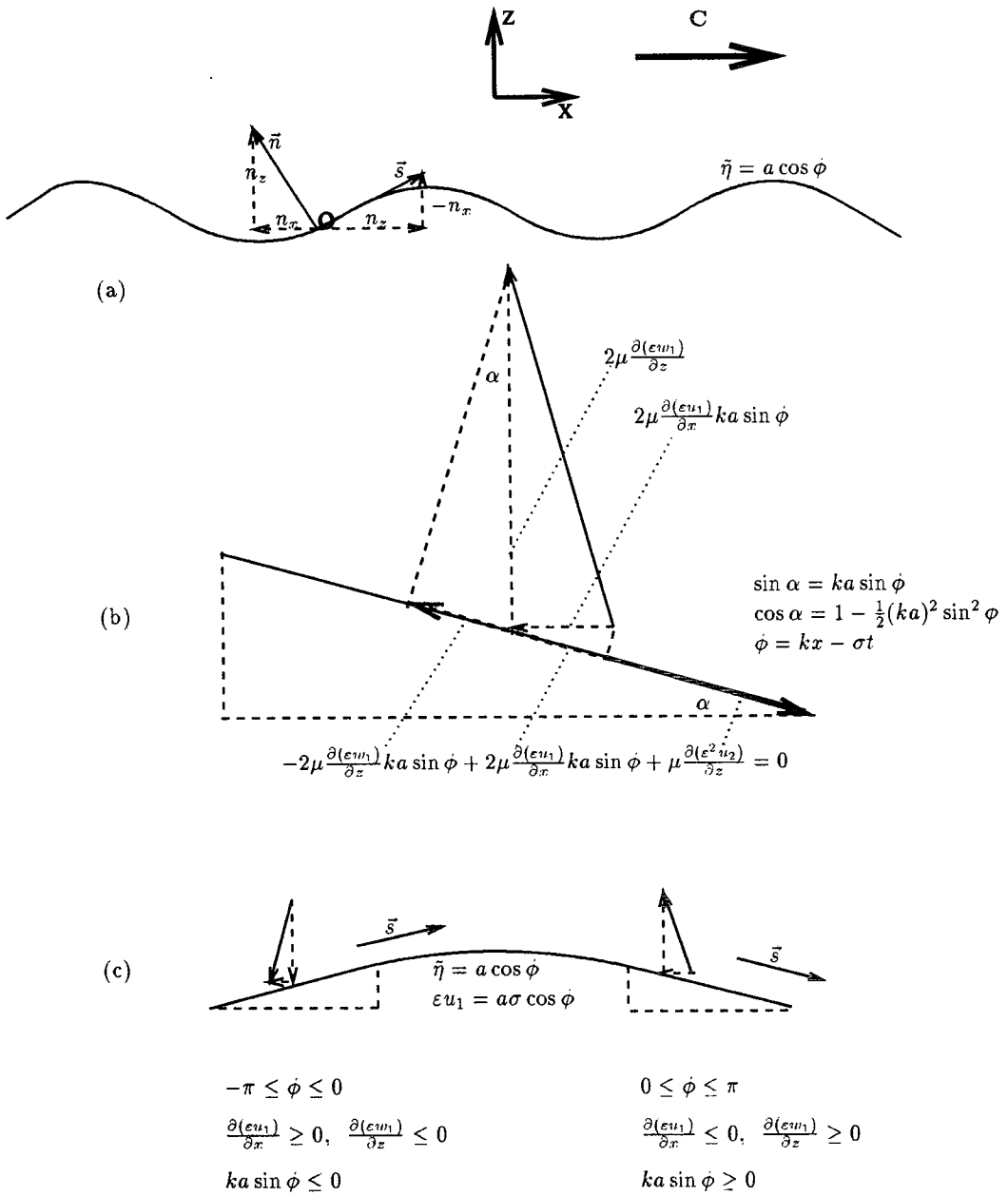

FIG. 3. (a) Normal and tangential directions on the free surface; (b) projections on the slope of two viscous normal stresses $2\mu ka\ \sin\theta(\partial u_1/\partial x)$ and $2\mu(\partial w_1/\partial z)$ acting on x and z planes, respectively; (c) the projections are always opposite to the tangential direction; when averaged over a wave cycle they contribute a second-order tangential stress, $\mu(\partial(\varepsilon^2 u_2)/\partial z)$, as is required by zero total tangential stress on the surface. In the figure, $\varepsilon = ka$, and we have used them alternatively.

When the earth's rotation is taken into account, there will be a wave crest parallel velocity component as is shown in section 2a. Consequently, the tensor P_{ij} will become three-dimensional ($i = x, y, z, j = x, y, z$). However, if the wave profile is unchanged along the direction of the crest as is assumed in section 2a (see also Fig. 2), the unit normal direction of the free surface is

$$\vec{n} = \left[ka\sin\phi,\ 0,\ 1 - \frac{1}{2}(ka)^2\sin^2\phi\right] \quad (49)$$

and the unit tangential direction is

$$\vec{s} = \left[1 - \frac{1}{2}(ka)^2\sin^2\phi,\ 0,\ -ka\sin\phi\right]. \quad (50)$$

Since both n_y and s_y are zero, neither P_{iy} nor P_{yj} can make a contribution to the tangential stress on the surface, whose formula is

$$P_{ns} = n_i P_{ij} s_j \quad (i = x, y, z, j = x, y, z). \quad (51)$$

Thus Eq. (45) remains formally valid. Substituting (7) into (45) we arrive at the same value for the virtual stress as is given by (48).

To estimate the size of the virtual tangential stress, we note that for sea waves the wave amplitude is statistically related to the frequency by

$$\frac{1}{2} a^2 = \int S(\sigma) d\sigma \quad (52)$$

in which $S(\sigma)$ is a wave energy spectrum. For the deep-water case, therefore, the virtual stress is the fifth moment of the energy spectrum,

$$\tau_{xz} = \frac{4\mu}{g^2} \int_0^\infty \sigma^5 S(\sigma) d\sigma, \quad (53)$$

where the deep-water dispersion relationship has been used. Thus the size of the virtual stress is entirely determined by the choices of μ and the form of the spectrum $S(\sigma)$. Longuet-Higgins (1969a,b) chose μ as molecular viscosity and the spectrum as

$$S(\sigma) = \alpha g^2 \sigma^{-5}, \quad \sigma_{\min} < \sigma < \sigma_{\max}, \quad (54)$$

where $\alpha = 1.2 \times 10^{-2}$ and the upper-limit frequency $\sigma_{\max}$ is related with the wind speed, and obtained

$$\tau_{xz} = 4\mu\alpha\sigma_{\max} \quad (55)$$

when $\sigma_{\max} \gg \sigma_{\min}$. Based on Cox's (1958) wind tunnel experiment data, he showed the ratio of the virtual wave stress to the wind stress decreases from 13% to 3% as the wind speed increases from 3.18 m s^{-1} to 12.02 m s^{-1}. As pointed out by Longuet-Higgins, this result assumes laminar motion; when laminar motion breaks down, the proportion of the virtual wave stress should be higher.

Madsen (1978) used the Pierson and Moskowitz (1964) spectrum and a wind velocity–related eddy viscosity to estimate the size of the surface velocity induced by the virtual wave stress in deep water. The size of the surface flow driven by the virtual stress he found is again on the same order as that driven purely by wind.

c. *Wave stress due to bottom friction*

The generation of the bottom streaming (Longuet-Higgins 1953) in a nonrotating frame was explained by Longuet-Higgins (1958): due to the existence of the bottom friction, the two wave orbital velocities, $\tilde{u}$ and $\tilde{w}$, are slightly in phase, resulting in a net Reynolds stress, $\langle \tilde{u}\tilde{w} \rangle$; this stress in turn drives the bottom streaming (also see Phillips 1977). Longuet-Higgins (1958) also showed that the bottom streaming, which was derived under the condition of constant viscosity in 1953, validates independently of the viscosity structure inside of the wave bottom friction layer. The bottom frictional layer is of order $O(\beta^{-1})$ thick, where $\beta = \sqrt{\sigma/2\nu}$. A more general model that allows the eddy viscosity varies both with time and the distance from the bottom was proposed by Trowbridge and Madsen (1984a,b).

The bottom streaming condition with rotation and viscous effects included has not been addressed previously, simply because attention has been focused on the case of infinitely deep water. In a rotating frame, there will be another bottom friction layer, which is of order $O(\delta_e)$, $\delta_e = \sqrt{2\nu/f}$. Since $\sigma \gg f$, the wave bottom friction layer is much thinner than the Ekman layer, the Ekman veering effect within this thin layer will be insignificant. In other words, we would expect that the introduction of the Coriolis force would have little effect on the wave stress within the thin wave boundary. The following detailed analysis confirms this expectation.

To examine the bottom wave stress in a rotating coordinate frame, one needs a solution for the primary wave motion of the real fluid near the bottom. To simplify the problem, we follow Longuet-Higgins' (1953) approach and take a constant viscosity. If both Coriolis force and vertical frictional force are retained in the momentum equations, the problem is still formidable. However, from the inviscid solution, we know that the wave crest parallel velocity component, $\tilde{v}$, is proportional to f/σ. Hence we can drop the Coriolis term in the x-momentum equation since it is of negligible order $O(f^2/\sigma^2)$. These simplifications allow us to consider the following equations first:

$$\left.\begin{aligned} \frac{\partial \tilde{u}}{\partial t} &= -\frac{1}{\rho}\frac{\partial \tilde{p}}{\partial x} + \nu \frac{\partial^2 \tilde{u}}{\partial z^2} \\ \frac{\partial \tilde{w}}{\partial t} + g &= -\frac{1}{\rho}\frac{\partial \tilde{p}}{\partial z} + \nu \frac{\partial^2 \tilde{w}}{\partial z^2} \\ \frac{\partial \tilde{u}}{\partial x} &+ \frac{\partial \tilde{w}}{\partial z} = 0 \end{aligned}\right\} \quad (56)$$

and then separately consider the solution for the $\tilde{v}$ component,

$$\frac{\partial \tilde{v}}{\partial t} + f\tilde{u} = \nu \frac{\partial^2 \tilde{v}}{\partial z^2}. \quad (57)$$

The solution of (56) together with nonslip bottom conditions and u approaching the inviscid solution in the interior region is straightforward (Phillips 1977), yielding

$$\tilde{u} = a\sigma \frac{\cosh kz'}{\sinh kh} \cos(kx - \sigma t) - a\sigma \frac{e^{-\beta z'}}{\sinh kh} \cos(kx - \sigma t + \beta z') \tag{58}$$

$$\tilde{w} = a\sigma \frac{\sinh kz'}{\sinh kh} \sin(kx - \sigma t) + \frac{a\sigma}{2} \left(\frac{k}{\beta}\right) \frac{1}{\sinh kh} \times [e^{-\beta z'} \cos(kx - \sigma t + \beta z') + e^{-\beta z'} \sin(kx - \sigma t + \beta z') - \cos(kx - \sigma t) - \sin(kx - \sigma t)]. \tag{59}$$

Knowing $\tilde{u}$, we can solve for $\tilde{v}$ in (57) to obtain

$$\tilde{v} = \left(\frac{f}{\sigma}\right) a\sigma \frac{\cosh kz'}{\sinh kh} \sin(kx - \sigma t) - \left(\frac{f}{\sigma}\right) a\sigma \frac{e^{-\beta z'}}{\sinh kh} \times \left[\sin(kx - \sigma t + \beta z') - \frac{1}{2} \beta z' \cos(kx - \sigma t + \beta z') + \frac{1}{2} \beta z' \sin(kx - \sigma t + \beta z')\right], \tag{60}$$

where we have used the notation

$$z' = z + h \tag{61}$$

$$\beta = \left(\frac{\sigma}{2\nu}\right)^{1/2} \tag{62}$$

and have neglected the terms of order $O(k^2/\beta^2)$. From (58) to (60), the wave stresses in the $x-$ and $y-$ directions are

$$\langle \tilde{u}\tilde{w} \rangle = \left(\frac{k}{\beta}\right) \frac{(a\sigma)^2}{4 \sinh^2 kh} [2\beta z' e^{-\beta z'} \sin \beta z' + 2e^{-\beta z'} \cos \beta z' - 1 - e^{-2\beta z'}] \tag{63}$$

$$\langle \tilde{v}\tilde{w} \rangle = \left(\frac{f}{\sigma}\right) \frac{(a\sigma)^2}{4 \sinh^2 kh} \sinh 2kz' - \left(\frac{f}{\sigma}\right) \frac{(a\sigma)^2}{4 \sinh^2 kh} e^{-\beta z'} \sinh kz' [2 \cos \beta z' + \beta z' \sin \beta z' + \beta z' \cos \beta z'] + \left(\frac{f}{\sigma}\right)\left(\frac{k}{\beta}\right) \frac{(a\sigma)^2}{4 \sinh^2 kh} [2e^{-\beta z'} \cos \beta z' - 1 - e^{-2\beta z'} + \beta z' e^{-\beta z'} \sin \beta z']. \tag{64}$$

The ratio of k to β can be expressed as

$$\frac{k}{\beta} = \frac{\sqrt{2\nu}}{g} \sigma^{3/2} \coth kh, \tag{65}$$

where the dispersion relationship $\sigma^2 = gk \tanh kh$ for the surface wave has been used. Typically, σ is of order 1 s^{-1} and the water depth h is not so shallow that $\coth kh$ is much larger than 1. Then k/β mainly depends on the choice of the viscosity ν. Typical values of ν for water ranges from 10^{-6} m^2 s^{-1} for molecular viscosity, to 10^{-2} m^2 s^{-1} for turbulent viscosity. Accordingly, $k/\beta = O(10^{-4}) \sim O(10^{-2})$. Thus, the ratio is a small number even for the turbulent conditions. Thus, kz' is always a small number compared with $\beta z'$ even when z' is away from the boundary layer. Hence

$$e^{-\beta z'} \sinh kz' \approx e^{-\beta z'} kz' = \frac{k}{\beta} e^{-\beta z'} \beta z'. \tag{66}$$

Therefore the second term on the right-hand side of (64) is $O[(fk)/(\beta\sigma)]$ like the last term, which is negligible. As a result, Eq. (64) is reduced to

$$\langle \tilde{v}\tilde{w} \rangle = \frac{f}{\sigma} \frac{(a\sigma)^2}{4 \sinh^2 kh} \sinh 2kz', \tag{67}$$

which is the same as the interior stress given by (12). Equation (63) is the same as that given by Phillips (1977), and we conclude that the earth's rotation does little to change the near-bottom stress distribution compared to that in a nonrotating system (Longuet-Higgins 1953, 1958; Phillips 1977).

From the above discussion, we now have a clear picture of the distribution of wave forcing. On the free surface, there is a wave-induced virtual tangential stress. In the interior region, there is a Coriolis-induced wave stress, whose distribution is concentrated mainly within a Stokes depth and is directed $\pi/2$ to the right of the wave propagation direction. At the bottom there is a wave stress in the same direction as the wave propagation; it arises from the phase shift of the orbital velocities across the bottom wave boundary layer.

3. Steady flow driven by winds and waves

a. General case

The wave forcing derived above is based on an assumption that the wave direction is along the x axis. Without difficulty, we can generalize the results to the case of arbitrary wave direction, θ, relative to the x

axis. Written in a complex plane, the wave body forcing in the water column including a thin bottom layer is

$$\tilde{A}\left[\frac{k}{\beta}\frac{\partial \tilde{X}}{\partial z}e^{i\theta}+\frac{f}{\sigma}\frac{\partial \tilde{Y}}{\partial z}e^{i(\theta-\pi/2)}\right],$$

where

$\tilde{A} = (a\sigma)^2$ wave stress amplitude in the water column

$\tilde{X} = \dfrac{1}{4\sinh^2 kh}(2\beta z' e^{-\beta z'}\sin\beta z' + 2e^{-\beta z'}\cos\beta z' - 1 - e^{-2\beta z'})$ the vertical profile of wave stress induced by the bottom friction

$\tilde{Y} = \dfrac{1}{4\sinh^2 kh}\sinh 2kz'$ the vertical profile of wave stress induced by Coriolis force,

and k is the wavenumber in the direction of θ. Also introduce the following notation:

$q = \langle u\rangle + i\langle v\rangle$ complex velocity

τ the amplitude of wind stress at the sea surface

$\tilde{\tau} = 2\mu\sigma k^2 a^2 \coth kh$ the amplitude of virtual tangential wave stress

ψ wind direction relative to the x axis

θ wave direction relative to the x axis

$q_{st}(-h) = \dfrac{\sigma a^2 k}{2\sinh^2 kh}$ Stokes velocity at the bottom.

Then the model for the steady flow driven by winds and waves can be written as

$$\nu\frac{\partial^2 q}{\partial z^2} - ifq = \tilde{A}\left[\frac{k}{\beta}\frac{\partial \tilde{X}}{\partial z}e^{i\theta}+\frac{f}{\sigma}\frac{\partial \tilde{Y}}{\partial z}e^{i(\theta-\pi/2)}\right] \quad (68)$$

subjected to

$$q = 0 \quad z' = 0 \quad (69)$$

$$\nu\frac{\partial q}{\partial z} = \frac{\tau}{\rho}e^{i\psi} + \frac{\tilde{\tau}}{\rho}e^{i\theta} \quad z' = h. \quad (70)$$

The solution can be written as the sum of the classical Ekman flow, q_1, the flow driven by Longuet-Higgins's two boundary conditions, q_2, and the flow driven by Coriolis-induced wave stress, q_3:

$$q_1 = \frac{\tau}{\rho f\delta_e}\sqrt{2}e^{i(\psi-\pi/4)}\frac{\sinh\alpha(h+z)}{\cosh\alpha h} \quad (71)$$

$$q_2 = \frac{\tilde{\tau}}{\rho f\delta_e}\sqrt{2}e^{i(\theta-\pi/4)}\frac{\sinh\alpha(h+z)}{\cosh\alpha h} + \frac{1}{2}q_{st}(-h)\left[3\frac{\cosh\alpha z}{\cosh\alpha h} + B(\beta z')\right]e^{i\theta} \quad (72)$$

$$q_3 = \left(\frac{a^2\sigma}{\delta_{st}}\right)e^{i(\theta-\pi)}F(z), \quad (73)$$

where we have used both z and z' for convenience, and

$$F(z) = \frac{1}{2+i\left(\frac{\delta_e}{\delta_{st}}\right)^2}\left\{\frac{\cosh 2k(h+z)}{2\sinh^2(kh)} - \frac{\cosh(\alpha z)}{2\sinh^2(kh)\cosh(\alpha h)} - \sqrt{2}e^{(-i\pi/4)}\left(\frac{\delta_e}{\delta_{st}}\right)\frac{\cosh(kh)}{2\sinh(kh)}\frac{\sinh\alpha(h+z)}{\cosh(\alpha h)}\right\}, \quad (74)$$

$$B(\beta z') = e^{-2\beta z'} - 2(\beta z'+2)e^{-\beta z'}\cos\beta z' - 2(\beta z'-1)e^{-\beta z'}\sin\beta z', \quad (75)$$

$$\delta_e = \left(\frac{2\nu}{f}\right)^{1/2} \quad (76)$$

$$\alpha = \frac{1+i}{\delta_e}, \quad (77)$$

and have neglected the terms $O(k\alpha^2/\beta^3)$.

The first part of q_2, similar in structure to the wind-driven Ekman flow q_1, is the Ekman flow driven by the virtual tangential wave stress. The second part of q_2 is the bottom streaming modified by the earth's rotation. As Fig. 4a [where $B(\beta z')$ is not plotted because it vanishes above the thin bottom wave boundary layer] shows, the introduction of the earth rotation restricts the flow in the two Ekman layers. The bottom Ekman layer flow is driven by the bottom streaming and the surface Ekman layer flow is driven by the virtual wave stress. In this case, the value of Stokes drift velocity at the bottom is -0.34, so the value of the bottom streaming is $-3/2 \times 0.34 = -0.51$.

There are two vertical scales in q_3. One is the Ekman depth, $\delta_e = \sqrt{2\nu/f}$, imposed internally by friction and Coriolis parameter. The other is the Stokes depth, $\delta_{st} = 1/(2k)$, which is imposed externally by the surface wave field (Fig. 4.b). The nature of q_3 critically depends on the ratio of δ_e/δ_{st}. When the ratio is infinitely large (which gives the nonrotating case), q_3 approaches zero.

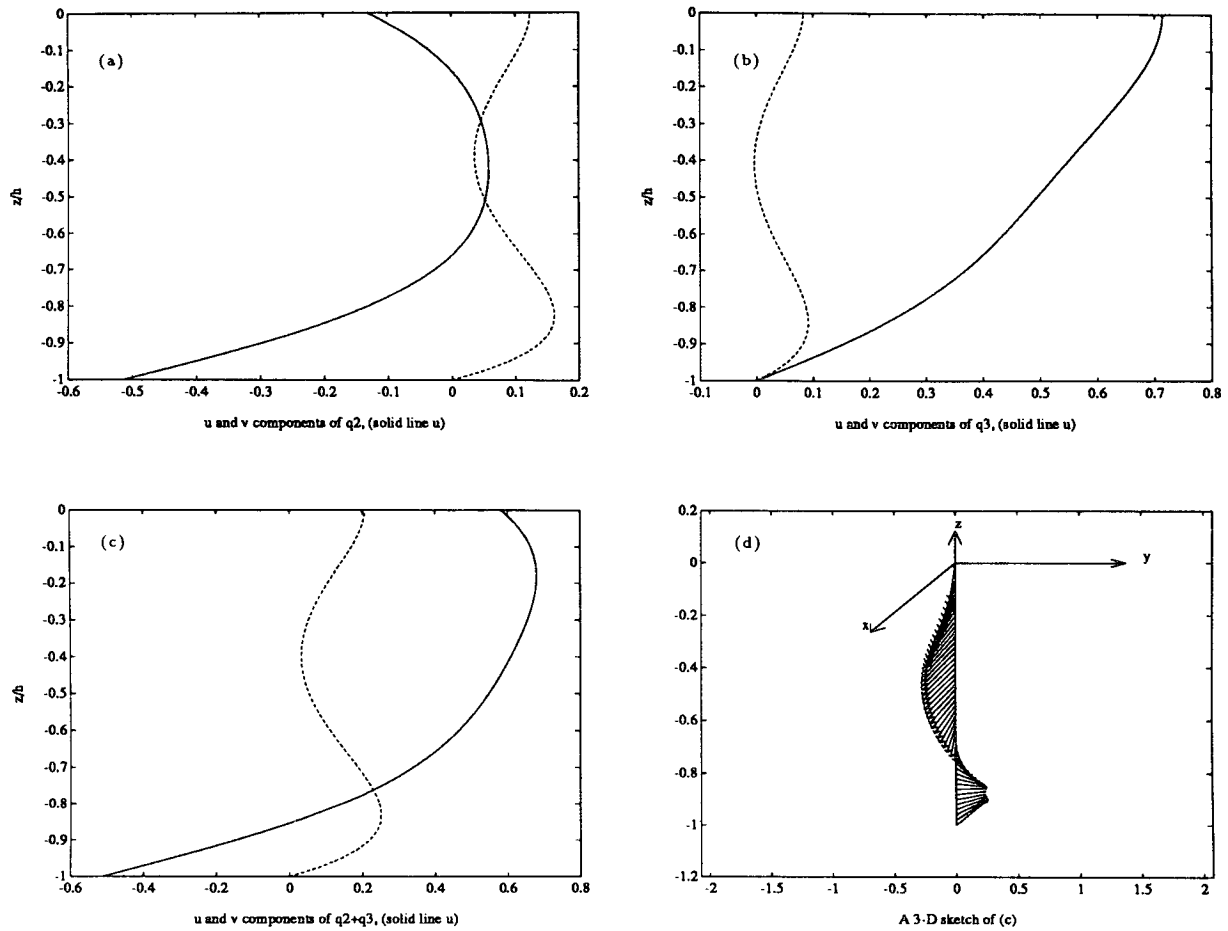

FIG. 4. The vertical structures of wave-driven steady flow, scaled by $a^2\sigma/\delta_{st}$. (a) Flow driven by viscous-induced wave stress. (b) Flow driven by Coriolis-induced wave stress. (c) Flow driven by both Coriolis- and viscous-induced wave stress, with (d) as its 3D sketch. The parameters are $h = 50$ m, $\delta_e/h = 0.23$, $\delta_{st}/h = 0.65$, $\theta = \pi$, which is toward minus x direction.

When the ratio approaches zero (which gives the inviscid case), q_3 becomes a return flow—an Eulerian flow of the same magnitude as the Stokes drift but with the opposite sign.

The summation of q_2 and q_3 provides an unified formula encompassing Longuet-Higgins's viscid but nonrotational theory and Ursell and Hasselmann's inviscid but rotational one,

$$q_{ws} = q_2 + q_3 = \frac{a^2\sigma}{\delta_{st}}\left[\frac{\sqrt{2}}{4}\frac{\delta_e}{\delta_{st}}\coth kh e^{i(\theta-\pi/4)}\frac{\sinh\alpha(h+z)}{\cosh\alpha h} + \frac{e^{i\theta}}{8\sinh^2 kh}\left(3\frac{\cosh\alpha z}{\cosh\alpha h} + B(\beta z')\right) + e^{i(\theta-\pi)}F(z)\right], \tag{78}$$

where we have used q_{ws} to denote wave-driven steady flow. We shall examine its various limiting cases next. Figure 4c shows the vertical structure of flow driven by both Coriolis- and viscosity-induced wave stresses, and Fig. 4d is its 3D sketch [again, $B(\beta z')$ is not plotted].

In comparison with the wind-driven flow, how large is the wave-driven flow? We notice that $\tilde{\tau}/(\rho f\delta_e) = ka^2\sigma(k\delta_e)$ and $a^2\sigma/\delta_{st} = 2ka^2\sigma$. While $ka^2\sigma$ is the amplitude of Stokes drift, with the usual value of about 10 cm s^{-1} (Bye 1967), and $k\delta_e$ is usually of order 1

(Madsen 1978; Weber 1983b). Therefore the wave-driven flow is of the order of 10 cm s^{-1}.

b. Some limiting cases for wave-driven flow

Here we focus on the discussion of some of the limiting cases for the steady wave-driven flow, q_{ws}.

• When $f \to 0$ and h is finite, then $\alpha \to 0$, $\delta_e \to \infty$, and

$$q_2 \to \left[\frac{\tilde{\tau}}{\mu}(h+z) + \frac{3}{2}q_{st}(-h)\right]e^{i\theta}. \quad (79)$$

$$F(z) \to 0. \quad (80)$$

Thus,

$$q_{ws} = \left[\frac{\tilde{\tau}}{\mu}(h+z) + \frac{3}{2}q_{st}(-h)\right]e^{i\theta}, \quad (81)$$

which, if added on the Stokes drift, recovers the Longuet-Higgins mass transport theory for a nonrotational viscid fluid.

Historically, Longuet-Higgins was the first one who obtained the virtual tangent stress. The algebra involved is complicated. Doubts were then raised by Huang (1970). He pointed out that the Longuet-Higgins formula for wave mass transport blows up when a deep-water limit is taken [as you can see from (81)]. This is the so-called Longuet-Higgins paradox. Ünlüata and Mei (1970) then reexamined the wave mass transport problem using a Lagrangian approach. Their result showed that the Longuet-Higgins result is indeed correct, given its underlying assumption that a steady state for the mass transport has been reached. The paradox arises because in a nonrotating system for deep water, the virtual surface wave stress remains unbalanced. Madsen (1978) then introduced the Coriolis force into the model to balance the virtual wave stress, successfully resolving the Longuet-Higgins paradox.

• The limit $f \to 0$ and $h \to \infty$ is an unfair case. This is equivalent to demanding that a steady state is achieved in an infinitely deep water as was originally demanded by Huang (1970).

• When $f \neq 0$ and $\nu \to 0$, then $\alpha \to \infty$, $\delta_e \to 0$, and

$$q_2 \to 0 \quad (82)$$

$$F(z) \to \frac{\cosh 2k(h+z)}{4\sinh^2(kh)}. \quad (83)$$

Thus

$$q_{ws} = -q_{st}e^{i\theta}, \quad (84)$$

which recovers Ursell's (1950) and Hasselmann's (1970) theory. The theory states that in a rotating inviscid ocean the Lagrangian mean flow must vanish. By adding Stokes drift velocity to the above Eulerian velocity, we obtain the required zero Lagrangian mean. Thus, our model yields a unified formula for the wave-driven flow in shallow water between viscid but nonrotational Longuet-Higgins theory and inviscid but rotational Ursell and Hasselmann's theory.

Equation (84) suggests a mechanism for generation of the wave-induced return flow. Traditionally the following explanation of the wave-induced return flow is given: a surface wave field produces a steady Stokes drift. When the drift hits a physical wall, water piles up there and a pressure gradient is generated that drives a return flow in the opposite direction to the wave propagation to compensate for the Stokes drift (Fig. 5). This mechanism crucially depends on the existence of the physical wall and it is quite hard to picture it in a region where the lateral boundary is far away. The Coriolis-induced wave force offers an alternative mechanism for generating the compensating return flow. As is indicated by (84), the Coriolis force–generated return flow is a depth-dependent mirror image of the Stokes drift, whereas a pressure force–generated return flow would be depth independent (Fig. 5b).

Equation (84) then predicts there will be a mean return flow component in a velocity time series recorded by any current meter (fixed in Eulerian space) where there are surface waves. Any attempt to explain the observed current dynamically without considering the surface wave effects may lead to wrong conclusions. We will discuss a possible example of this later.

• When $h \to \infty$

$$F(z) \to \frac{1}{2 + i(\delta_e/\delta_{st})^2}\left[e^{2kz} - \frac{\sqrt{2}}{2}e^{(-i\pi/4)}\left(\frac{\delta_e}{\delta_{st}}\right)e^{\alpha z}\right] \quad (85)$$

$$q_2 \to \frac{\tilde{\tau}}{\rho f \delta_e}\sqrt{2}e^{i(\theta-\pi/4)}e^{\alpha z} \quad (86)$$

$$q_{ws} = \frac{a^2\sigma}{\delta_{st}}e^{i(\theta-\pi)}\left[\frac{e^{2kz} - \frac{\sqrt{2}}{2}e^{(-i\pi/4)}\left(\frac{\delta_e}{\delta_{st}}\right)e^{\alpha z}}{2 + i\left(\frac{\delta_e}{\delta_{st}}\right)^2}\right] + \frac{\tilde{\tau}}{\rho f \delta_e}\sqrt{2}e^{i(\theta-\pi/4)}e^{\alpha z}, \quad (87)$$

which, if added on Stokes drift, recovers Madsen's (1978) deep-water solution in Lagrangian form.

4. Unsteady flow driven by waves

We now investigate unsteady wave-driven flow. First, we consider the transient solution to a suddenly imposed steady wave forcing, and second, the response to varying wave forcing.

a. Transient solution for a suddenly imposed steady wave forcing

Denote q' as the transient response to a suddenly imposed steady wave forcing. The total response is then

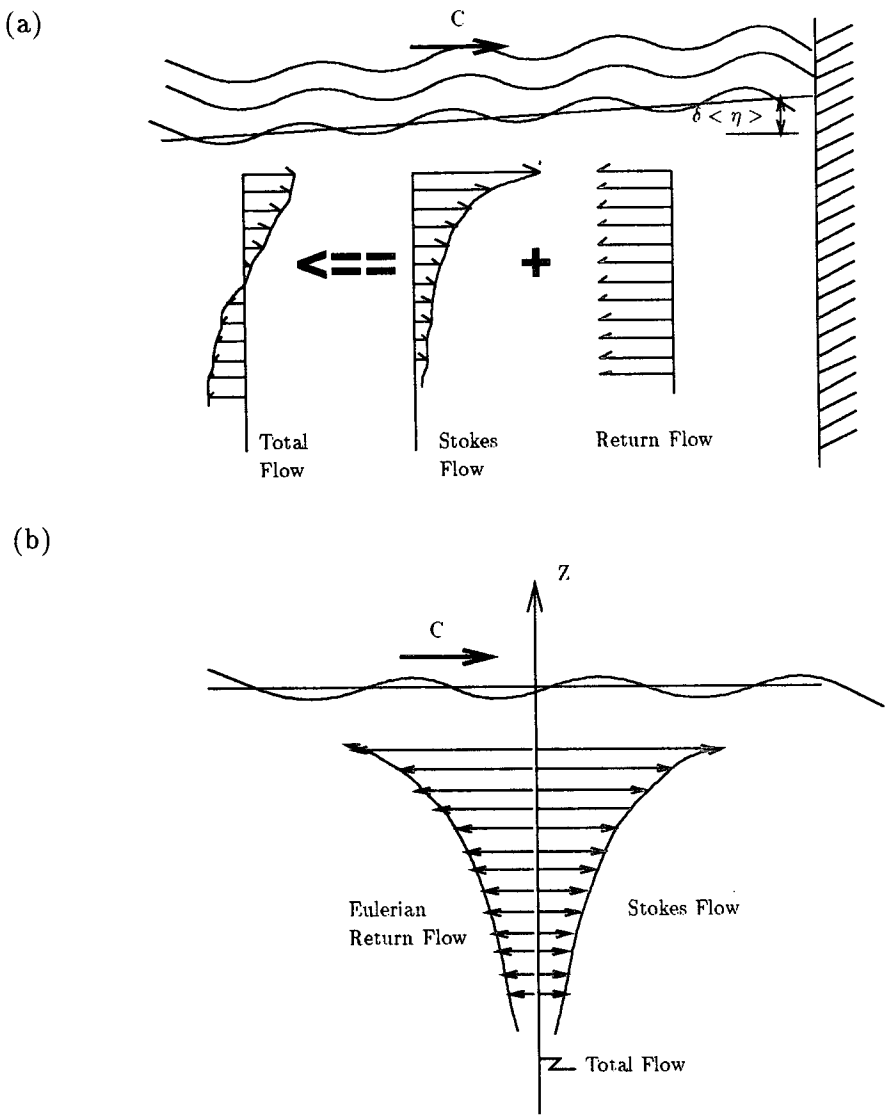

FIG. 5. (a) A traditional explanation for wave-induced return flow—a physical wall blocking the wave-induced Stokes drift is a necessity for generating return flow. (b) Another explanation for wave-induced return flow—return flow can be generated without lateral boundary, and the vertical distribution is a mirror image of the Stokes flow for the case of no friction.

the sum of q' and the steady solution q_{ws}, which we have already obtained as in (78). The transient response is governed by

$$\nu \frac{\partial^2 q'}{\partial z^2} - ifq' - \frac{\partial q'}{\partial t} = 0 \tag{88}$$

$$q' = 0 \quad z = -h \tag{89}$$

$$\nu \frac{\partial q'}{\partial z} = 0 \quad z = 0 \tag{90}$$

$$q' = -q_{ws} \quad t = 0 \quad \text{and} \quad -h < z < 0. \tag{91}$$

This is an eigenvalue problem in space with

$$\cos(\omega_n z), \tag{92}$$

$$\omega_n = \frac{2n+1}{2h}\pi \tag{93}$$

$$(n = 0, 1, 2, 3, \cdots) \tag{94}$$

as its eigenfunctions and eigenvalues, respectively. The transient solution is found to be

$$q' = \sum_{n=0}^{\infty} C_n e^{-(\gamma_n^2 + i)ft} \cos(\omega_n z), \tag{95}$$

where γ_n is given by

$$\gamma_n = \omega_n\left(\frac{\nu}{f}\right)^{1/2} \tag{96}$$

$$\overset{or}{=} \frac{1}{\sqrt{2}}\left(\frac{2n+1}{2}\pi\right)\left(\frac{\delta_e}{h}\right); \tag{97}$$

C_n can be determined from the initial condition; that is,

$$-q_{ws} = \sum_{n=0}^{\infty} C_n \cos(\omega_n z), \tag{98}$$

which gives

$$C_n = -\frac{2}{h}\int_{-h}^{0} q_{ws}\cos(\omega_n z)dz, \tag{99}$$

and the further computation is not included here.

The total solution, say, q_w, is then

$$q_w = q_{ws} + \sum_{n=0}^{\infty} C_n e^{-(\gamma_n^2+i)ft}\cos(\omega_n z). \tag{100}$$

Figure 6 shows different views of the development of the flow driven by a steady wave. Panels (a) and (b) show the development of vertical profiles of u and v. The profiles start from zero in the interior region, gradually accelerate, oscillate at the inertial frequency and finally settle down to the steady responses (where the most dense lines) on a momentum diffusion time scale of $(h/\delta_e)^2$. The final nonzero value of u at the bottom is the bottom streaming just above the thin wave bottom boundary layer (which is not plotted there). Panels (c) and (d) are time series of the surface values of u and v. Figure 5e is the hodograph of u versus v at different depths.

When $h \to \infty$, (95) and (99) are replaced by

$$q' = \int_0^{\infty} C(\omega)e^{-(if+\omega^2\nu)t}\cos(\omega z)d\omega \tag{101}$$

in which

$$C(\omega) = -\frac{2}{\pi}\int_{-\infty}^{0} q_{ws}\cos(\omega z)dz. \tag{102}$$

The deep-water transient solution may be rewritten as

$$q' = -e^{-ift}\int_{-\infty}^{\infty} q_{ws}(z-z')\frac{e^{-z'^2/4\nu t}}{\sqrt{4\pi\nu t}}dz', \tag{103}$$

since

$$\int_0^{\infty} C(\omega)\cos(\omega z)d\omega = -q_{ws} \tag{104}$$

$$\int_0^{\infty} e^{-\omega^2\nu t}\cos(\omega z)d\omega = \frac{1}{2}\left(\frac{\pi}{\nu t}\right)^{1/2} e^{-z^2/4\nu t}. \tag{105}$$

The total solution for deep water is then

$$q_w = q_{ws} - e^{-ift}\int_{-\infty}^{\infty} q_{ws}(z-z')\frac{e^{-z'^2/4\nu t}}{\sqrt{4\pi\nu t}}dz'. \tag{106}$$

When ν approaches zero,

$$\lim_{\nu\to 0}\frac{e^{-z^2/4\nu t}}{\sqrt{4\pi\nu t}} = \delta(z), \tag{107}$$

where $\delta(z)$ is the Dirac delta function, and q_{ws} approaches minus q_{st} as described by (84). Therefore (106) becomes

$$q_w = [-q_{st} + e^{-ift}q_{st}]e^{i\theta}, \tag{108}$$

which recovers Hasselmann's (1970) inertial oscillation solution in an inviscid deep ocean. Hasselmann proposed the Coriolis-induced wave force as a new generation mechanism against those of tidal generation and wind generation for the inertial oscillations often observed in the open ocean.

b. *Solution for unsteady wave forcing*

Notice that the wave forcing is related to a^2. Therefore, when the forcing is unsteady, we can multiply the squared wave amplitude by a time-dependent function, say $\zeta(t)$. In a small time step $\Delta t'$, the forcing increment is proportional to $\partial\zeta(t')/\partial t\Delta t'$; hence the corresponding water response increment is

$$\frac{\partial\zeta(t')}{\partial t}q_w(t-t')\Delta t'. \tag{109}$$

If the initial response is zero, the summation of all these small increments amounts to the total water response to the time varying forcing,

$$q = \int_0^t \frac{\partial\zeta(t')}{\partial t}q_w(z, t-t')dt', \tag{110}$$

where q_w is given by (100) [or (106) if the water depth is infinite].

For a suddenly imposed steady forcing, we have

$$\zeta(t) = H(t), \tag{111}$$

where $H(t)$ is the Heaviside step function with the definition as

$$H(t) = \begin{cases} 1, & \text{when } t \geqslant 0 \\ 0, & \text{when } t < 0 \end{cases} \tag{112}$$

and one of its properties is

$$\frac{\partial H(t)}{\partial t} = \delta(t), \tag{113}$$

substitution of which into (110) immediately recovers the response, q_w, to the suddenly imposed steady forcing.

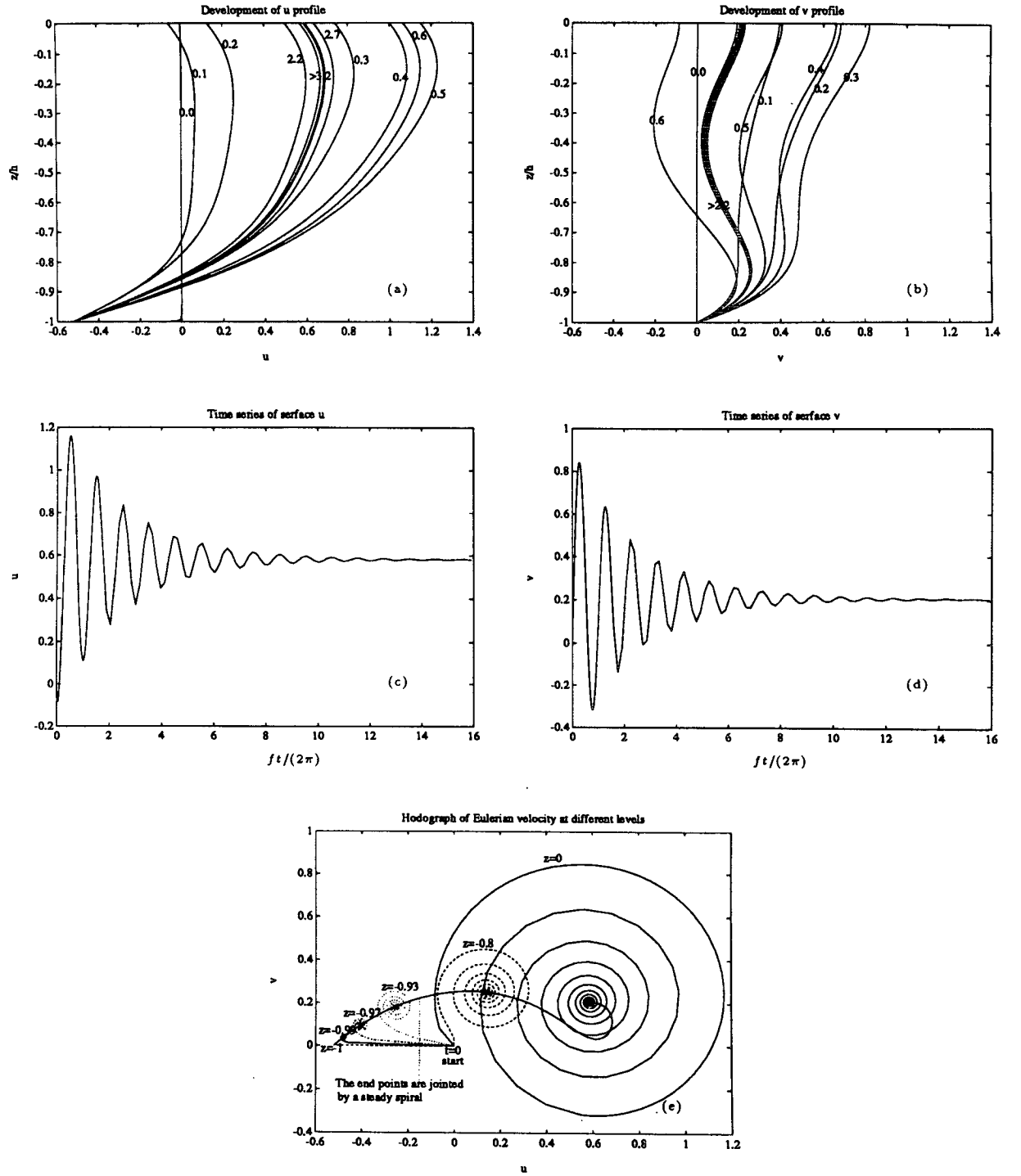

FIG. 6. Different views on the flow development driven by a steady wave ($\delta_e/h = 0.23$, $\delta_{st}/h = 0.65$, $\theta = \pi$). The numbers beside the curves in (a) and (b) are the values of $ft/(2\pi)$. The velocity is scaled by the strength of Stokes drift, $a^2\sigma/\delta_{st}$.

For a suddenly imposed wave and afterward subjected to decay due to both internal friction and bottom friction, we have

$$\zeta(t) = H(t)e^{-(4\nu k^2 + \nu\beta k/\sinh 2kh)t} \qquad (114)$$

[this energy dissipation rate can be worked out by substitution of (58) and (59) into (124) and retaining the leading terms in interior and bottom regions, respectively (also see Phillips 1977, pp. 52–53), whereby

$$\frac{\partial \zeta(t)}{\partial t} = \left[\delta(t) - \left(4\nu k^2 + \frac{\nu\beta k}{\sinh 2kh}\right)H(t)\right] \times e^{-(4\nu k^2 + \nu\beta k/\sinh 2kh)t}. \quad (115)$$

The time-varying form of the wave energy given in (114) validates for wave decay due to a molecular viscosity or due to a constant eddy viscosity. When wave breaking processes exist, the form of $\zeta(t)$ is subject to great uncertainty, and how to seek a proper form is beyond the scope of this paper. We notice that this problem has been recently addressed by Weber and Melson (1993a). The idea there is that although the form of $\zeta(t)$ for breaking waves is difficult to obtain, the wave heights before and after breaking and the time duration for the breaking process may be known, say, from experiments. Thus, one can calculate $\Delta\zeta(t)/\Delta t$ for approximation to $\partial\zeta(t)/\partial t$. As we can see from (110) that it is the time derivative of $\zeta(t)$ not $\zeta(t)$ itself that matters for the time-varying wave-driven flow.

The above analysis is for a monochromatic and unidirectional wave field. However, since the model in question is linear, we can sum up the different responses to the different wave frequencies and directions when the wave field is random. All we need to do is to replace a^2 in (78) by

$$2S(\sigma, \theta)d\sigma d\theta,$$

where $S(\sigma, \theta)$ is the wave energy directional spectrum, and then integrate (78) over a suitable range of frequencies and directions. The results described by (100), (106), and (110) will formally remain the same.

5. Comments on the need to include wave stress

In many of the coastal wind-driven circulation experiments the Coriolis term in the alongshore momentum equation is found to be dynamically large but uncorrelated with the other first-order terms (Allen and Smith 1981; Pettigrew 1981; Lentz and Winant 1986; Masse 1988; Lee et al. 1989). The data listed in Table 1 is cited from Lentz and Winant to illustrate this imbalance.

The problem has been attributed to instrumental noise (Lentz and Winant 1986) and to small-scale alongshore pressure gradients (Pettigrew 1981) but still remains a puzzle. The Coriolis-induced wave stress may offer a partial explanation for the imbalance. Generally, near the coast there is a shoreward propagating wave component. According to (84), there will be an Eulerian return flow in the water column. The recorded current will certainly include this return flow, while the external forcing, the surface wave field, responsible for this flow would not normally be included in these experiments; hence an apparent imbalance arises. A wave of 10 sec period and 1.26 m amplitude is sufficient to account for the uncorrelated term $f\{u\} = 5 \times 10^{-5}$ m^2 s^{-2} in Table 1. This suggests a need for the studies of shelf dynamics to include wave forcing, which has usually been neglected.

TABLE 1. Alongshore momentum imbalance in a coastal experiment (Lentz and Winant 1986). The notation { } means depth integration, F means the divergence of the alongshore component of the horizontal Reynolds stress, and the others should be self-explanatory.

Terms	Magnitude (10^{-5} m^2 s^{-2})
$\{v\}_t$	5
$\{uv\}_x$, $\{v^2\}_y$	1
$f\{u\}$	$\leqslant$5
$gH\eta_y$	5
$\left\{\int_z^{\eta'} \frac{g}{\rho_0}\frac{\partial \rho}{\partial y}\,dz'\right\}$	1
$\frac{\tau^s}{\rho_0}$	5
$\frac{\tau^b}{\rho_0}$	5
$\{F\}$	0.2

The wave forcing has an interesting dependence on bottom topography. This is reflected in two aspects. One is that the function $\sinh kh$ (or the like) explicitly appears in the wave forcing. Another is the wave shoaling and refraction processes that a train of waves will experience, since the wave phase velocity and group velocity are a function of water depth. Both of the processes will result in a change in wave height. The wave heights directly affect the size of wave forcing as can be seen above. The refraction process also will result in a tendency for the wave front to become parallel with the depth contours. Therefore, taking a circular bump on an otherwise flat bottom as an example, when a train of waves passes the bump, there will be concentration of wave forcing above the bump, and moreover, even if the bump is symmetrical in its geometry, the concentration of the wave forcing will generally be asymmetrical because the waves usually propagate through the bump from one side to the other. In contrast, the wind forcing is totally independent of the sea bottom topography. Further exploration of this unique feature of wave forcing may be interesting.

6. Summary and discussion

Wave forcing has been examined for a rotating viscous fluid of finite depth. A simple Eulerian model is presented to accommodate the wave forcing in addition to wind forcing. The model yields a general formula for the wind- and wave-driven flow for both steady and unsteady forcing, for arbitrary water depth and arbitrary wave direction. The solution for wave-driven steady flow recovers the Longuet-Higgins (1953) wave mass transport theory in the limit $f \to 0$, and recovers

Ursell's (1950) and Hasselmann's (1970) zero mean theory when the limit $\nu \to 0$ is taken; in the deep-water limit, it becomes the Eulerian counterpart of the Madsen Lagrangian solution in deep water.

The effect of surface waves on the mean flow is twofold. One is a wave-induced body force distributed mainly within a Stokes depth from the surface. It arises from rotation. The second one is the wave-induced virtual shear stress at the sea surface and wave-induced streaming at the bottom, due to the fluid viscosity. By adopting an Eulerian viewpoint, we can easily incorporate these two wave effects into classical fluid problem as demonstrated by the present discussion. In the course of validating the Longuet-Higgins virtual tangent stress in a rotating system, we found a succinct way to rigorously rederive the stress and thereby revealed its essence. The virtual tangent stress is the projection on the surface slope of the two viscous normal stresses acting on x and z planes, respectively.

The size of the wave-driven flow is typically comparable with that driven by winds. When the sea becomes very rough, the wave-driven flow can be very significant. With inclusion of the wave stress, some problems confronting us such as alongshore momentum imbalance found in many coastal experiments of wind-driven circulation may be resolved.

The solutions obtained here are local solutions in the same sense that the Ekman transport due to the wind is a local result. In deeper water, the inviscid solution in which the Stokes drift is exactly balanced by an upwave Eulerian current (Fig. 5b) provides a reasonable first approximation for the solution including viscosity. However, the inclusion of the viscous terms leads to a net transport in both downwave and alongcrest direction. In infinitely deep water the fluxes (only in alongcrest direction) are small compared to typical Ekman transports (Weber and Melson 1993b). However, in finite depth the transports associated with the bottom boundary layer become increasingly important (Fig. 4), giving significant depth-integrated flows in the wave direction and to the right of the wave direction (in the Northern Hemisphere). A full regional solution then needs a mass balance condition imposed by the appropriate boundary conditions. There is the possibility of strong local flows associated, for example, with large swell propagating over complex shallow topography, analogous to the rip currents in nearshore circulation patterns.

Acknowledgments. The authors wish to thank Dr. D. Wright for his very thorough review of this manuscript and his valuable comments. The research was supported by the Natural Sciences and Engineering Research Council of Canada.

APPENDIX

Wave Energy Dissipation and Virtual Tangential Stress in the Rotating System

We follow Phillips's wave energy dissipation approach to examine the Longuet-Higgins virtual tangential stress in a rotating system. Since we are particularly concerned with the viscous effects near the boundary, let us introduce a vertical shear stress, $\partial\tau_{xz}/\partial z$, into the x-momentum equation as

$$\frac{\partial \tilde{u}}{\partial t} - f\tilde{v} = -g\frac{\partial \tilde{\eta}}{\partial x} + \frac{1}{\rho}\frac{\partial \tau_{xz}}{\partial z}. \tag{116}$$

Integrating the above equation from $z = 0$ to $z = \tilde{\eta}$, and then phase averaging, we obtain

$$\frac{\partial \langle \tilde{u}\tilde{\eta}\rangle}{\partial t} - \langle \tilde{u}\tilde{w}\rangle - f\langle \tilde{v}\tilde{\eta}\rangle = -\frac{1}{\rho}\langle \tau_{xz}\rangle \quad \text{at} \quad z = 0, \tag{117}$$

where we have used

$$\bullet \left\langle \int_0^{\tilde{\eta}} \frac{\partial \tilde{u}}{\partial t}\, dz \right\rangle \approx \left\langle \tilde{\eta}\frac{\partial \tilde{u}}{\partial t}\right\rangle\Big|_{z=0}$$

$$= \frac{\partial \langle \tilde{u}\tilde{\eta}\rangle}{\partial t} - \left\langle \tilde{u}\frac{\partial \tilde{\eta}}{\partial t}\right\rangle \quad z = 0$$

$$= \frac{\partial \langle \tilde{u}\tilde{\eta}\rangle}{\partial t} - \langle \tilde{u}\tilde{w}\rangle \quad z = 0; \tag{118}$$

$$\bullet \left\langle \int_0^{\tilde{\eta}} f\tilde{v}\, dz \right\rangle \approx f\langle \tilde{v}\tilde{\eta}\rangle \quad z = 0; \tag{119}$$

- there is no horizontal variation[1] in wave amplitude, so that $\langle \frac{1}{2} g\partial\tilde{\eta}^2/\partial x\rangle = 0$;
- $\tau_{xz} = 0$ at the real surface.

According to (7)–(11), $\tilde{u}$ and $\tilde{w}$ are in quadrature and so are $\tilde{v}$ and $\tilde{\eta}$. Thus (117) is reduced to

$$\frac{\partial \langle \tilde{u}\tilde{\eta}\rangle}{\partial t} = -\frac{1}{\rho}\langle \tau_{xz}\rangle. \tag{120}$$

From (7) to (11), one can calculate the total wave energy per area below the plane $z = 0$, denoted as E, to be

$$E = (2k)^{-1}\rho a^2\sigma^2 \coth kh, \tag{121}$$

where the high-order terms of $O(f^2/\sigma^2)$ have been neglected. From (7) to (11), one can also verify that

$$\rho\langle \tilde{u}\tilde{\eta}\rangle|_{z=0} = \frac{k}{\sigma}E, \tag{122}$$

whereby

$$\rho\frac{\partial \langle \tilde{u}\tilde{\eta}\rangle}{\partial t}\Big|_{z=0} = \frac{k}{\sigma}\frac{\partial E}{\partial t}. \tag{123}$$

[1] This assumption is made to simplify the discussion. The classical wave radiation stress (Longuet-Higgins and Stewart 1960) will take care of the term $\langle \frac{1}{2} g\partial\tilde{\eta}^2/\partial x\rangle$, if there is horizontal inhomogeneity in the wave amplitude.

For the plane wave in question the energy dissipation rate per unit area is given by

$$\frac{\partial E}{\partial t} = -\mu \int_{-h}^{0} \left\{ 2\left\langle \left(\frac{\partial \tilde{u}}{\partial x}\right)^2 \right\rangle + 2\left\langle \left(\frac{\partial \tilde{w}}{\partial z}\right)^2 \right\rangle + \left\langle \left(\frac{\partial \tilde{u}}{\partial z} + \frac{\partial \tilde{w}}{\partial x}\right)^2 \right\rangle + \left\langle \left(\frac{\partial \tilde{v}}{\partial x}\right)^2 \right\rangle + \left\langle \left(\frac{\partial \tilde{v}}{\partial z}\right)^2 \right\rangle \right\} dz, \quad (124)$$

from which we can see that the energy dissipation rate associated with the strain in v will be of order of f^2/σ^2; hence we can omit it in the calculation. Substituting (7) to (9) into the above expression, we have

$$\frac{\partial E}{\partial t} = -2\mu a^2 \sigma^2 k \coth kh. \quad (125)$$

Thus from (117)

$$\tau_{xz} = -\rho \frac{\partial \langle \tilde{u}\tilde{\eta} \rangle}{\partial t} = -\frac{k}{\sigma}\frac{\partial E}{\partial t} = 2\mu\sigma k^2 a^2 \coth kh. \quad (126)$$

A second-order motion then is set up on $z = 0$ to balance this shear stress; that is,

$$\mu \frac{\partial \langle u \rangle}{\partial z} = 2\mu\sigma k^2 a^2 \coth kh. \quad (127)$$

REFERENCES

Allen, J. S., and R. L. Smith, 1981: On the dynamics of wind-driven shelf currents. *Philos. Trans. Roy. Soc. London,* **A302,** 617–634.

Andrews, D. G., and M. E. McIntyre, 1978: An exact theory of nonlinear waves on a Lagrangian-mean flow. *J. Fluid Mech.,* **89**(4), 609–646.

Bye, J. A. T., 1967: The wave drift current. *J. Mar. Res.,* **25,** 95–102.

Grant, W., A. Williams, and S. Glenn, 1984: Bottom stress estimates and their prediction on the northern California continental shelf during code-1: The importance of wave–current interaction. *J. Phys. Oceanogr.,* **14,** 506–527.

Hasselmann, K., 1970: Wave-driven inertial oscillations. *Geophys. Fluid Dyn.,* **1,** 463–502.

Huang, N. E., 1970: Mass transport induced by wave motion. *J. Mar. Res.,* **29,** 35–50.

Jenkins, A. D., 1986: A theory for steady and variable wind- and wave-induced currents. *J. Phys. Oceanogr.,* **16,** 1370–1377.

——, 1987a: Wind and wave induced currents in a rotating sea with depth-varying eddy viscosity. *J. Phys. Oceanogr.,* **17,** 938–951.

——, 1987b: A Lagrangian model for wind- and wave-induced near-surface currents. *Coastal Eng.,* **11,** 513–526.

——, 1989: The use of a wave prediction model for driving a near-surface current model. *Dtsch. Hydrogr. Z.,* **42,** 133–149.

Lee, T. N., E. Williams, J. Wang, and R. Evans, 1989: Response of South Carolina continental shelf waters to wind and Gulf Stream forcing during winter of 1986. *J. Geophys. Res.,* **94**(C8), 10 715–10 754.

Lentz, C. D., and S. J. Winant, 1986: Subinertial currents on the southern California shelf. *J. Phys. Oceanogr.,* **16,** 1737–1750.

Longuet-Higgins, M. S., 1953: Mass transport in water waves. *Philos. Trans. Roy. Soc.,* **A245,** 535–581.

——, 1958: The mechanics of the boundary-layer near the bottom in a progressive wave. [Appendix to R. C. H. Russell and J. D. C. Osorio, "An experimental investigation of drift profiles in a closed channel."] *Proc. Sixth Conf. on Coastal Engineering,* Berkeley, Council on Wave Research, University of California, 171–193.

——, and R. W. Stewart, 1960: Changes in the form of short gravity waves on long waves and tidal currents. *J. Fluid Mech.,* **8,** 565–583.

——, 1969a: On the transport of mass by time-varying ocean currents. *Deep-Sea Res.,* **16,** 431–447.

——, 1969b: A nonlinear mechanism for the generation of sea waves. *Proc. Roy. Soc. London,* **A311,** 371–389.

Madsen, O. S., 1978: Mass transport in deep water waves. *J. Phys. Oceanogr.,* **8,** 1009–1015.

Masse, A. K., 1988: Estuary–shelf interaction: Delaware Bay and inner shelf. Ph.D. thesis, University of Delaware, 216 pp.

Pierson, W. J., and L. Moskowitz, 1964: A proposed spectral form for fully developed wind seas based on the similarity theory of S. A. Kitaigorodskii. *J. Geophys. Res.,* **69,** 5181–5190.

Pettigrew, N. R., 1981: The dynamics and kinematics of the coastal boundary layer off Long Island. Ph.D. thesis, Woods Hole Oceanographic Institution, 262 pp.

Phillips, O. M., 1977: *The Dynamics of The Upper Ocean,* 2d ed. Cambridge University Press, 261 pp.

Pollard, R. T., 1970: Surface waves with rotation: An exact solution. *J. Geophys. Res.,* **75,** 5895–5898.

Stokes, G. G., 1847: On the theory of oscillatory waves. *Trans. Camb. Phil. Soc.,* **8,** 441–455.

Trowbridge, J., and O. S. Madsen, 1984a: Turbulent wave boundary layers 1. Model formulation and first-order solution. *J. Geophys. Res.,* **89**(C5), 7989–7997.

——, and ——, 1984b: Turbulent wave boundary layers 2. Second-order theory and mass transport. *J. Geophys. Res.,* **89**(C5), 7999–8007.

Ünlüata, Ü., and Mei, 1970: Mass transport in water waves. *J. Geophys. Res.,* **75,** 7611–7618.

Ursell, F., 1950: On the theoretical form of ocean swell on a rotating earth. *Mon. Not. Roy. Astron. Soc., Geophys. Suppl.,* **6,** 1–8.

Weber, J. E., 1983a: Steady wind- and wave-induced currents in the open ocean. *J. Phys. Oceanogr.,* **13,** 524–530.

——, 1983b: Attenuated wave-induced drift in a viscous rotating ocean. *J. Fluid Mech.,* **137,** 115–129.

——, 1990: Eulerian versus Lagrangian approach to wave-drift in a rotating ocean. *Acta Geophys.,* **3,** 155–170.

——, and A. Melson, 1993a: Volume flux induced by wind and waves in a saturated sea. *J. Geophys. Res.,* **98**(C3), 4739–4745.

——, and ——, 1993b: Transient ocean currents induced by wind and growing waves. *J. Phys. Oceanogr.,* **23,** 193–206.